JVI Journals.ASM.org

Virus-Induced Tubule: a Vehicle for Rapid Spread of Virions through Basal Lamina from Midgut Epithelium in the Insect Vector

Dongsheng Jia,[a] Qianzhuo Mao,[a] Hongyan Chen,[a] Aiming Wang,[b] Yuyan Liu,[a] Haitao Wang,[a] Lianhui Xie,[a] Taiyun Wei[a]

Fujian Province Key Laboratory of Plant Virology, Institute of Plant Virology, Fujian Agriculture and Forestry University, Fuzhou, Fujian, People's Republic of China[a]; Southern Crop Protection and Food Research Centre, Agriculture and Agri-Food Canada, London, Ontario, Canada[b]

ABSTRACT

The plant reoviruses, plant rhabdoviruses, tospoviruses, and tenuiviruses are transmitted by insect vectors in a persistent propagative manner. These viruses induce the formation of viral inclusions to facilitate viral propagation in insect vectors. The intestines of insect vectors are formed by epithelial cells that lie on the noncellular basal lamina surrounded by visceral muscle tissue. Here, we demonstrate that a recently identified plant reovirus, southern rice black-streaked dwarf virus (SRBSDV), exploits virus-containing tubules composed of virus-encoded nonstructural protein P7-1 to directly cross the basal lamina from the initially infected epithelium toward visceral muscle tissues in the intestine of its vector, the white-backed planthopper (*Sogatella furcifera*). Furthermore, such tubules spread along visceral muscle tissues through a direct interaction of P7-1 and actin. The destruction of tubule assembly by RNA interference with synthesized double-stranded RNA targeting the P7-1 gene inhibited viral spread in the insect vector *in vitro* and *in vivo*. All these results show for the first time that a virus employs virus-induced tubule as a vehicle for viral spread from the initially infected midgut epithelium through the basal lamina, facilitating the rapid dissemination of virus from the intestine of the insect vector.

IMPORTANCE

Numerous plant viruses are transmitted in a persistent manner by sap-sucking insects, including thrips, aphids, planthoppers, and leafhoppers. These viruses, ingested by the insects, establish their primary infection in the intestinal epithelium of the insect vector. Subsequently, the invading virus manages to transverse the basal lamina, a noncellular layer lining the intestine, a barrier that may theoretically hinder viral spread. The mechanism by which plant viruses cross the basal lamina is unknown. Here, we report that a plant virus has evolved to exploit virus-induced tubules to pass through the basal lamina from the initially infected midgut epithelium of the insect vector, thus revealing the previously undescribed pathway adapted by the virus for rapid dissemination of virions from the intestine of the insect vector.

Transmission by insect vectors is essential for the infection cycle of numerous viruses that cause diseases in humans, animals, and plants. The hemipteran insects, including aphids, whiteflies, leafhoppers, and planthoppers, are global pests and vectors that transmit numerous plant viruses in a persistent manner. The intestine of hemipteran insects is formed by epithelial cells that lie on the noncellular basal lamina surrounded by the visceral muscle tissues (1, 2). For the insect vector to persistently transmit the virus, virions move from the intestine to other organs or the salivary glands, where they are finally released to plant hosts (3–5). Thus, virions must pass through the basal lamina of the intestine into the hemolymph (3–5). The basal lamina of hemipteran insects is a tightly interwoven and noncellular matrix (3, 4), constituting a substantial barrier for viral persistent transmission. How free plant virions cross the intestinal basal lamina of the insect vectors is unknown. The mechanism by which plant viruses are able to move from the intestinal epithelium across the basal lamina into the hemolymph and, finally, the salivary glands is critical to our understanding of persistent modes of transmission and, ultimately, to the development of control strategies.

The plant reoviruses, plant rhabdoviruses, tospoviruses, and tenuiviruses are persistently transmitted and propagate during infection of their vectors (3–5). These viruses replicate and induce the formation of various inclusions to facilitate viral propagation in the insect vectors (3–5). For example, plant reoviruses replicate within cytoplasmic viral inclusions called viroplasms that are composed of viral nonstructural proteins in the insect vectors (6–10). Recently, we have shown that a tenuivirus, rice stripe virus, exploits viral inclusions constructed by the nonstructural protein NS4 to facilitate viral spread in the body of the small brown planthopper (*Laodelphax striatellus*) (11). Furthermore, a plant reovirus, rice dwarf virus (RDV), uses virus-containing tubules composed of the nonstructural protein Pns10 for trafficking along the microvilli and visceral muscles of the intestine, facilitating viral spread within its vector, the green rice leafhopper (*Nephotettix cincticeps*) (12–15). We thus hypothesized that the tubules induced by plant reoviruses might play a critical role in viral dissemination across the intestinal basal lamina, carrying the virus to the visceral muscle tissues and effectively establishing systemic infection in the insect vectors.

In this study, we chose a recently identified plant reovirus, southern rice black-streaked dwarf virus (SRBSDV), as a model

Received 1 May 2014 **Accepted** 19 June 2014
Published ahead of print 25 June 2014
Editor: A. Simon
Address correspondence to Taiyun Wei, weitaiyun@fjau.edu.cn.
D.J. and Q.M. contributed equally to this article.

doi:10.1128/JVI.01261-14

virus to study the mechanism by which plant viruses exploit virus-induced tubules to mediate viral dissemination from the intestine of the insect vectors. SRBSDV, a tentative species of the genus *Fijivirus* in the family *Reoviridae*, was first reported in Guangdong Province, China, in 2001 and has spread throughout southern China and northern Vietnam via the transmission by the white-backed planthopper (WBPH; *Sogatella furcifera* Horváth) (16–19). After ingestion of viral particles by the WBPH, SRBSDV first enters the epithelial cells of the midgut, where viroplasms composed of nonstructural proteins P5, P6, and P9-1 are formed for viral replication and assembly of progeny virions (9, 10, 20). Subsequently, SRBSDV crosses the midgut basal lamina in an as yet uncharacterized way into the hemolymph and then, finally, into the salivary glands (10, 20). Here, we demonstrate that SRBSDV has evolved a mechanism to exploit virus-containing tubules composed of viral nonstructural protein P7-1 to cross the midgut basal lamina from the initially infected epithelial cells toward visceral muscle tissues, mediating viral dissemination from the intestine of its insect vector.

MATERIALS AND METHODS

Cell, virus, and antibodies. Continuous cultures of the vector cell in monolayer (VCM) were developed from WBPH cells and maintained on the growth medium as described previously (9, 10). SRBSDV was purified from infected cultured WBPH cells as described previously (21). VCMs on coverslips were inoculated with a virus preparation as described previously (9). The SRBSDV isolate was maintained on rice plants via transmission by the WBPH as reported previously (16, 18, 20). Polyclonal antibodies against the nonstructural proteins P7-1 and P9-1 of SRBSDV were prepared as reported in a recent study (10). IgGs isolated from polyclonal antibodies against nonstructural proteins P7-1 and P9-1 of SRBSDV were conjugated to fluorescein isothiocyanate (FITC) or rhodamine (Invitrogen) according to the manufacturer's instructions.

Double labeling of P7-1 and actin in VCMs during infection by SRBSDV. Synchronous infection of VCMs by SRBSDV was initiated as described previously (9, 10). VCMs growing on a coverslip were inoculated with SRBSDV at a high multiplicity of infection (MOI) of 10. At 84 h postinoculation (hpi), VCMs were fixed, immunolabeled with P7-1-specific IgG conjugated to rhodamine (P7-1-rhodamine) and the actin dye FITC-phalloidin (Invitrogen), and then processed for immunofluorescence microscopy as already described (6, 10). As controls, the mock-infected VCMs were treated exactly in the same way.

Examination of SRBSDV infection in VCMs in the presence of synthesized dsRNAs. A 1,074-bp segment of the P7-1 gene of SRBSDV and the 717-bp segment of the green fluorescent protein (GFP) gene were amplified by PCR. A T7 RiboMAX Express RNA interference (RNAi) system kit (Promega) was used to synthesize *in vitro* double-stranded RNAs (dsRNAs) for these two genes according to the manufacturer's instructions. To examine the effects of synthesized dsRNAs targeting either the GFP gene (dsGFP) or the P7-1 gene (dsP7-1) on viral spread, VCMs were transfected with 0.5 μg/μl dsRNAs in the presence of the Cellfectin reagent (Invitrogen) for 24 h and then inoculated with SRBSDV at a low MOI of 0.04. At 36 or 84 hpi, VCMs were fixed, immunolabeled with P9-1-specific IgG conjugated to FITC (P9-1–FITC) and P7-1–rhodamine, and then processed for immunofluorescence microscopy, as described previously (12, 13).

We examined the effects of the synthesized dsGFP or dsP7-1 on viral replication by transfecting the VCMs with dsRNAs and then inoculating them with SRBSDV at an MOI of 10. At 84 hpi, VCMs were fixed, immunolabeled with P9-1–FITC and P7-1–rhodamine, and then visualized by immunofluorescence microscopy. At 84 hpi, the infected cells were collected, and the titer of cell-associated viruses in the cell lysates was determined by using a fluorescent focus assay, as described previously (22). At 84 hpi, the accumulation of P7-1 and P9-1 of SRBSDV in the cell lysates was further analyzed using a Western blotting assay with P7-1- and P9-1-specific IgGs, respectively. WBPH actin was detected with actin-specific IgG (Sigma).

Immunofluorescence labeling of internal organs of WBPHs after acquisition of SRBSDV. Fifty second-instar nymphs of the WBPH were fed on diseased rice plants for 1 day and then transferred to healthy rice seedlings. At different days following viral acquisition by WBPHs, internal organs from 50 WBPHs were dissected, fixed, immunolabeled with P9-1–FITC, P7-1–rhodamine, and the actin dye phalloidin-Alexa Fluor 647 carboxylic acid (Invitrogen), and then processed for immunofluorescence microscopy, as described previously (12, 13). As controls, the internal organs dissected from WBPHs which were fed on healthy rice plants were treated exactly in the same way.

Effects of synthesized dsRNAs on viral accumulation and transmission by WBPHs. The dsRNAs were microinjected into WBPHs following the method reported for the brown planthopper (23). Briefly, 50 third-instar nymphs of the WBPH were fed on SRBSDV-infected rice plants for 1 day. Then, individual nymphs were microinjected with 200 nl dsGFP or dsP7-1 (0.5 μg/μl) at the conjunction site between the prothorax and the mesothorax (23) and then kept on healthy rice plants. At 2 and 6 days post-first access to diseased plants (padp), we dissected the internal organs from 50 WBPHs that had received dsRNAs. The internal organs of the insects were dissected, fixed, and then processed for immunofluorescence microscopy. At 6 days padp, the accumulation of P7-1 and P9-1 of SRBSDV was analyzed by Western blotting assay with P7-1- and P9-1-specific IgGs, respectively.

To determine whether the microinjection of dsRNAs affected the transmission of SRBSDV by the insect vectors, 100 WBPH nymphs were fed on SRBSDV-infected rice plants for 1 day, microinjected with 200 nl dsP7-1 or dsGFP (0.5 μg/μl), and then kept on healthy rice seedlings for 14 days. Individual WBPH adults were then fed on healthy rice seedlings in individual tubes for 2 days. The rice plants were tested for visible symptoms.

Immunoelectron microscopy. Virus-infected VCMs on coverslips or the intestines from viruliferous WBPHs were fixed, dehydrated, and embedded, and thin sections were cut as described previously (6, 14). Sections were then incubated with P7-1-specific or actin-specific IgGs (Sigma) and immunogold labeled with goat antibodies against rabbit IgG that had been conjugated with 10- or 15-nm-diameter gold particles (Sigma) (6, 14).

Yeast two-hybrid assay. A yeast two-hybrid assay was performed using a DUALmembrane starter kit (Dualsystems Biotech) according to the manufacturer's instructions. Briefly, the P7-1 gene of SRBSDV and the actin gene of the WBPH were cloned into the bait vector PBT-STE and the prey vector PPR3-N, respectively. The recombinant plasmids PBT-STE-P7-1 and PPR3-N-actin, pBT3-STE-P7-1 and pPR3-N, or pBT3-STE and pPR3-N-actin were cotransformed with *Saccharomyces cerevisiae* yeast strain NMY51. Plasmids pTSU2-APP and pNubG-Fe65 as positive controls or pPR3-N as a negative control were cotransformed into NMY51. All transformants were grown on synthetic dropout (SD)-Trp-Leu-His-Ade agar plates for 3 to 4 days at 30°C.

Pulldown assay. The P7-1 gene of SRBSDV and the GFP gene were cloned into pET30a for fusion with the His tag. The actin gene of the WBPH was cloned into PGEX-3× for fusion with glutathione *S*-transferase (GST). All recombinant proteins were expressed in *Escherichia coli* strain BL21. GST-actin was incubated with glutathione-Sepharose beads (Amersham) for 4 h at 4°C. His–P7-1 or His-GFP was added to the beads, and the mixture was incubated for 4 h at 4°C. The beads were collected and washed with wash buffer (300 mM NaCl, 10 mM Na_2HPO_3, 2.7 mM KCl, 1.7 M KH_2PO_4). Immunoprecipitated proteins were detected using a Western blotting assay with His-tagged and GST-tagged antibodies (Sigma), respectively.

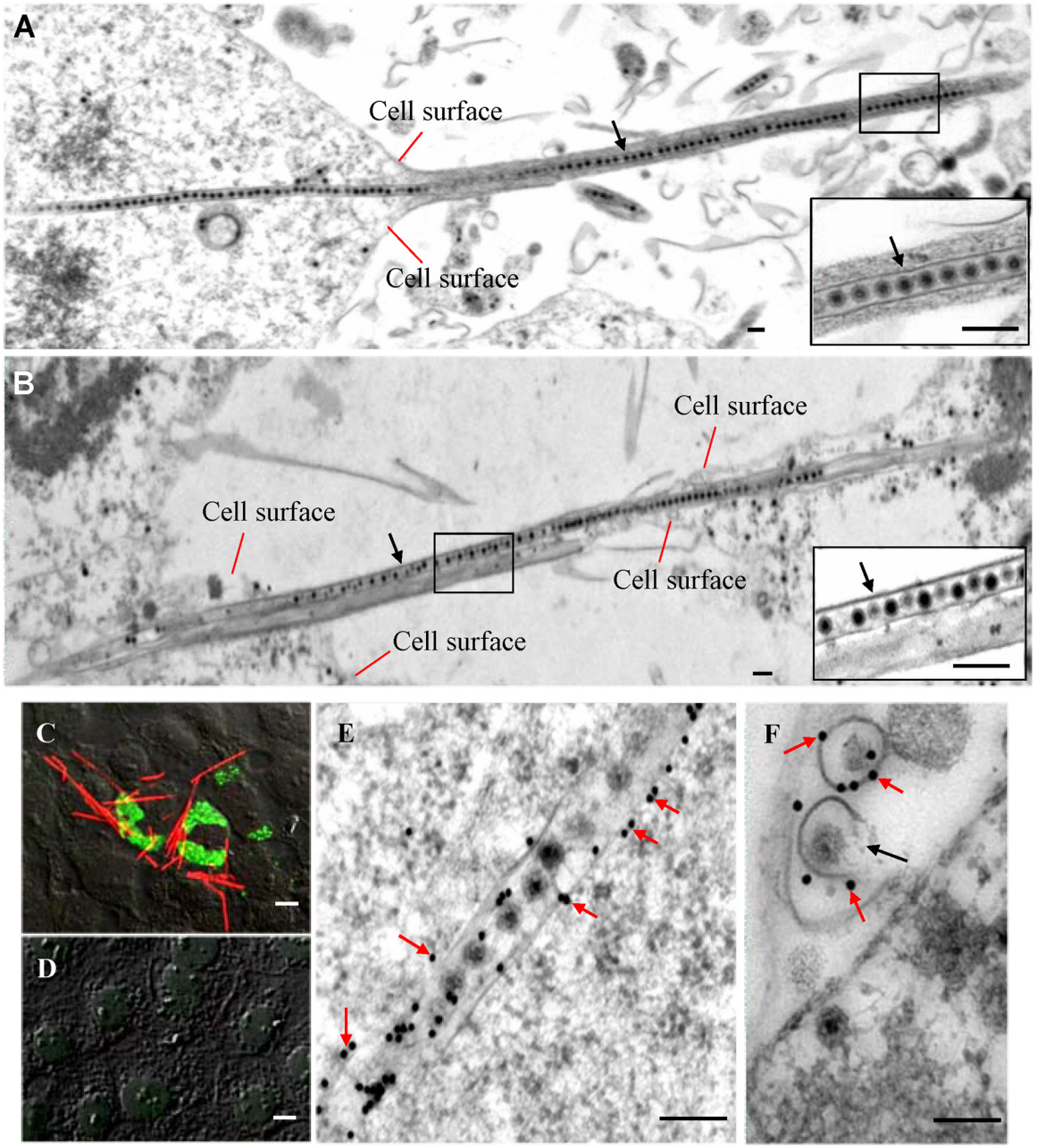

FIG 1 Tubules were formed by nonstructural protein P7-1 of SRBSDV in virus-infected VCMs. (A, B) Electron micrographs of the virus-containing tubules (arrows) protruding from the cell surface to connect neighboring cells at 84 hpi. (Insets) Enlarged images of the boxed areas. Bars, 100 nm. (C, D) Confocal immunofluorescence micrographs of the tubules protruding from the surface of infected cells at 84 hpi. SRBSDV-infected (C) and mock-infected (D) VCMs were immunolabeled with P9-1–FITC (green) and P7-1–rhodamine (red). Bars, 5 μm. (E, F) Immunogold labeling of P7-1 of SRBSDV in the tubules in longitudinal (E) or transverse (F) sections at 84 hpi. Cells were immunolabeled with P7-1-specific IgG as the primary antibody, followed by treatment with 15-nm gold particle-conjugated goat antibodies against rabbit IgG as secondary antibodies. Black arrow in panel F, an incompletely closed tubule. Bars, 100 nm.

RESULTS

The nonstructural protein P7-1 of SRBSDV forms cytoplasmic tubules in insect vector cells. Examination of thin sections of SRBSDV-infected VCMs derived from WBPHs at 84 hpi by electron microscopy revealed that virions were arranged in tubules approximately 85 nm in diameter in the cytoplasm or protruding from the surface of the WBPH cells (Fig. 1A). These virus-containing tubules extended into the actin-based cell protrusions, namely, the filopodia, from infected cells toward neighboring cells (Fig. 1A and B). In an earlier study, we showed that the viral nonstructural protein P7-1 alone (in the absence of viral infection) has the intrinsic ability to form tubules that are approximately 85 nm in diameter and extend from the cell surface of insect Sf9 cells (24). Furthermore, P7-1 of SRBSDV and Pns10 of RDV, both of which are major constituents of the tubules induced by these two plant reoviruses, appear to have similar secondary

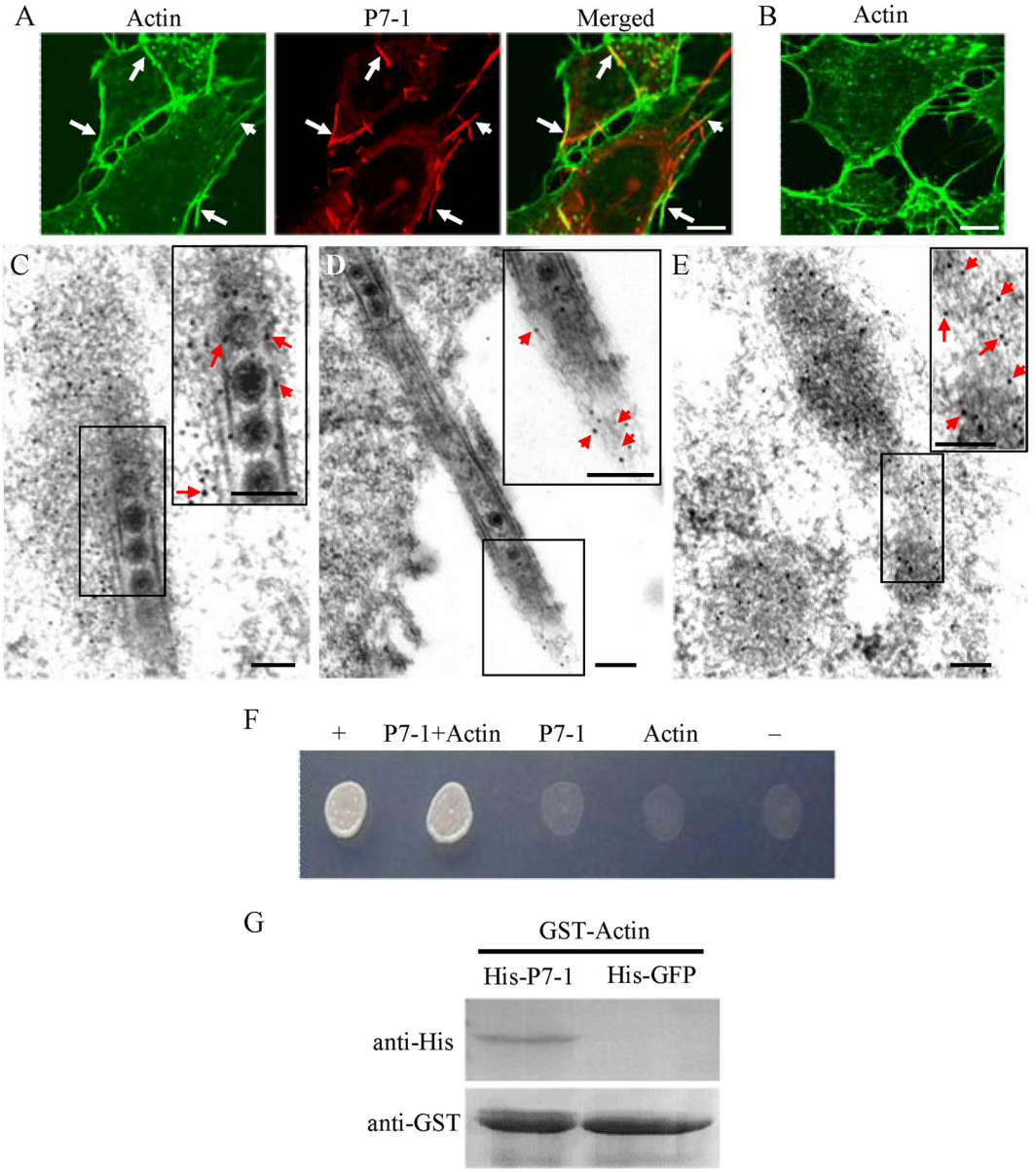

FIG 2 Association of P7-1 tubules with actin filaments in VCMs. (A, B) Immunofluorescence micrographs of the colocalization of P7-1 tubules with actin filaments (arrows) in VCMs at 84 hpi. SRBSDV-infected (A) and mock-infected (B) VCMs were immunolabeled with the actin dye FTIC-phalloidin (green) and P7-1–rhodamine (red). Bars, 5 μm. (C to E) Immunoelectron micrographs of the association of some actin filaments with virus-containing tubules within the cytoplasm (C) or along the filopodia (D) at 84 hpi. SRBSDV-infected (C, D) and mock-infected (E) VCMs were immunolabeled with actin-specific IgG as the primary antibody, followed by treatment with 10-nm gold particle-conjugated goat antibodies against rabbit IgG as secondary antibodies. (Insets) Enlarged images of the boxed areas. Arrows, gold particles. Bars, 100 nm. (F) The interaction between P7-1 of SRBSDV and actin of the WBPH detected by yeast two-hybrid assay. Transformants on an SD-Trp-Leu-His-Ade agar plate are shown. +, positive control, i.e., pBT3-STE and pOst1-NubI; P7-1+Actin, pBT3-STE-P7-1 and pPR3-N-actin; P7-1, pBT3-STE-P7-1 and pPR3-N; Actin, pBT3-STE and pPR3-N-actin; −, negative control, i.e., pBT3-STE and pPR3-N. (G) The pulldown assay was used to detect the interaction between P7-1 of SRBSDV and actin of WBPH. P7-1 of SRBSDV was fused with His to act as a bait protein with GFP as a control. Actin of WBPH was fused with GST as a prey protein. Actin bound to His-fused P7-1 of SRBSDV, but it did not bind to His-fused GFP.

structures with a conserved assembly strategy (12–15, 24). To explore the function of the P7-1 tubules, we used immunofluorescence microscopy to determine the subcellular distribution of P7-1 and the viroplasm matrix protein P9-1 of SRBSDV by immunolabeling with P7-1–rhodamine and P9-1–FITC at 84 hpi. The results indicated that P7-1 of SRBSDV was present in numerous tubule-like structures protruding from the surface of infected cells (Fig. 1C). No specific fluorescence was detected in mock-infected cells after immunolabeling with P7-1–rhodamine and P9-1–FITC (Fig. 1D). Immunoelectron microscopy confirmed that virus-containing tubules were immunolabeled with P7-1-specific IgG (Fig. 1E and F). Furthermore, some P7-1 tubules were incompletely closed and morphologically appeared like a scroll (Fig. 1F), suggesting that they were assembling the complete closed tubules. These data suggest that P7-1 of SRBSDV is responsible for the formation of the tubules and that the extension of

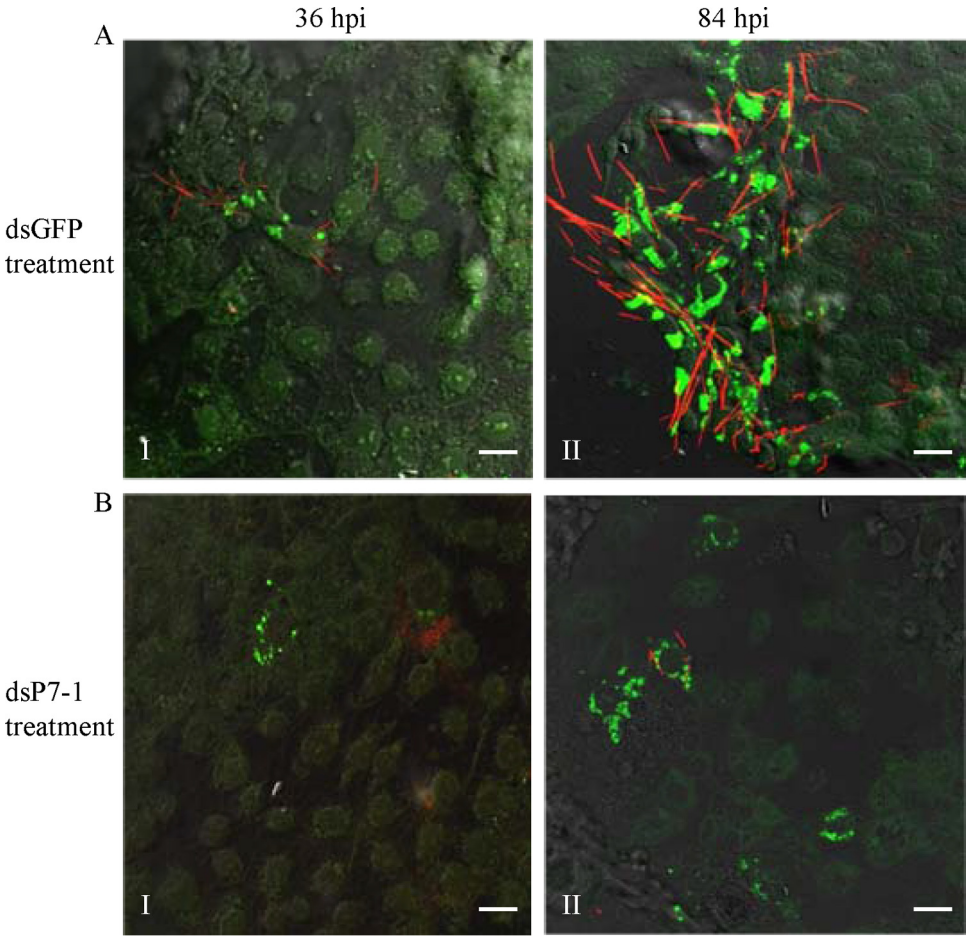

FIG 3 RNAi induced by dsP7-1 inhibited the assembly of tubules and the spread of SRBSDV in VCMs. At 24 h after transfection with dsGFP (A) or dsP7-1 (B), VCMs were inoculated with SRBSDV at an MOI of 0.04. At 36 hpi (panels I) or 84 hpi (panels II), VCMs were immunolabeled with P9-1–FITC (green) and P7-1–rhodamine (red) and then examined by confocal microscopy. Images are representative of those from more than 4 experiments. Bars, 20 μm.

these tubules from the cell surface does not require other components harbored by SRBSDV (24).

P7-1 tubules associate with the actin cytoskeleton in insect vector cells. To examine how P7-1 tubules associate with actin-based filopodia in virus-infected VCMs, we used immunofluorescence microscopy to visualize the tubules in VCMs during infection by SRBSDV. Our results showed that some P7-1 tubules colocalized with actin filaments within the cytoplasm or on the filopodia (Fig. 2A and B). Immunoelectron microscopy confirmed that actin filaments were closely associated with virus-containing tubules within the cytoplasm or along the filopodia (Fig. 2C to E). The association of P7-1 tubules with actin filaments seemed not to cause the reorganization of actin filaments compared with the organization of actin filaments in mock-infected cells (Fig. 2A to E).

The DUAL membrane system, a variant of the yeast two-hybrid assay, was used to determine whether there is a protein-protein interaction between P7-1 of SRBSDV and actin of the WBPH. Our results indicated that P7-1 of SRBSDV interacted directly with actin of the WBPH (Fig. 2F). To further confirm this interaction, P7-1 of SRBSDV was tested for the interaction with actin of the WBPH using a pulldown assay. The results showed that the GST-fused actin of the WBPH specifically bound to His-fused P7-1 of SRBSDV but did not bind to His-fused GFP (the negative bait control) (Fig. 2G). All these results suggest that the association of P7-1 tubules with filopodia is mediated by a specific interaction between P7-1 and actin of the WBPH in virus-infected VCMs.

RNAi induced by synthesized dsRNAs targeting the P7-1 gene inhibits tubule formation and viral spread among insect vector cells. To determine whether P7-1 tubules play a crucial role in viral spread, VCMs were treated with dsRNAs targeting the P7-1 gene. At 24 h after treatment, the treated VCMs were inoculated with SRBSDV at a low MOI of 0.04. At this low MOI, the early viral infection rate was low, and the spread of virus among insect vector cells could be easily monitored. At 36 hpi, SRBSDV infection was restricted to a limited number of the initially infected cells in the presence of dsGFP or dsP7-1 (Fig. 3A and B, panels I). By this time point, it was evident that the formation of P7-1 tubules had been significantly inhibited by the treatment with dsP7-1 (Fig. 3B, panel I). At 84 hpi, viral infection was spread in an extensive area of VCMs that were treated with dsGFP (Fig. 3A, panel II). However, in VCMs that were treated with dsP7-1, viral infection was still restricted to a limited area of VCMs (Fig. 3B, panel II). Thus, our results suggest that the inhibition of

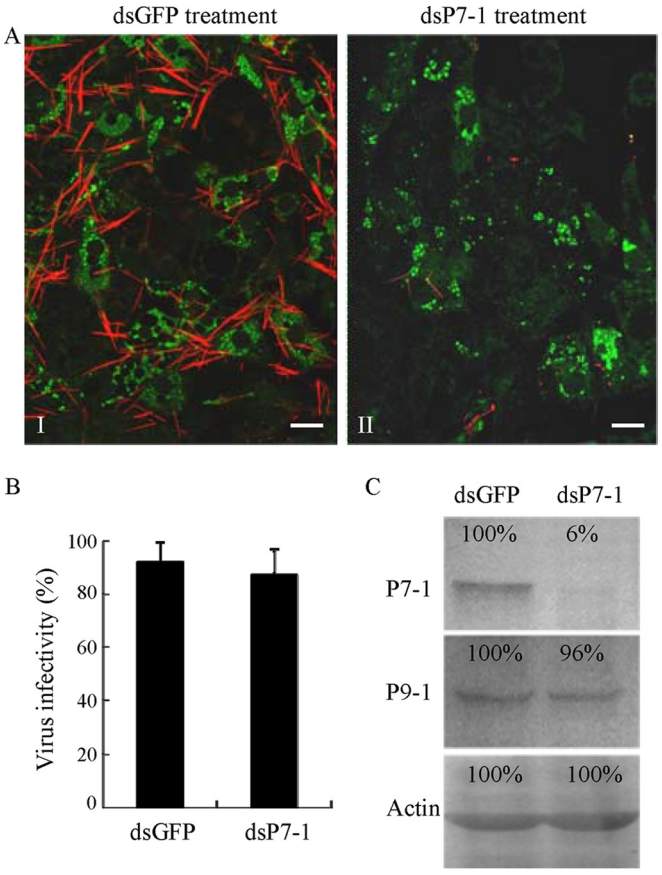

FIG 4 RNAi induced by dsP7-1 knocks down the expression of P7-1 without significantly inhibiting virus replication in VCMs. (A) dsP7-1 did not significantly affect the viral infection rate in VCMs. VCMs were transfected with dsGFP (panel I) or dsP7-1 (panel II) and then inoculated with SRBSDV at an MOI of 10. At 84 hpi, cells were immunolabeled with P9-1–FITC (green) and P7-1–rhodamine (red) and then examined by confocal microscopy. Images are representative of those from more than 4 experiments. Bars, 20 μm. (B) Effect of treatment with dsRNAs on the accumulation of cell-associated SRBSDV in VCMs at 84 hpi. Viral titers were determined in duplicate by a fluorescent focus assay. Error bars indicate standard deviations from three independent experiments. (C) A Western blotting assay showed that dsP7-1 significantly reduces the accumulation of P7-1 but not P9-1 of SRBSDV in virus-infected VCMs at 84 hpi. Proteins were separated by SDS-PAGE to detect P7-1 or P9-1 with P7-1- or P9-1-specific IgGs, respectively. Insect actin was detected with actin-specific IgG as a control. The protein accumulation level in VCMs transfected with dsGFP was taken to be 100%.

P7-1 tubule formation reduces the spread of SRBSDV from the initially infected cells.

To further investigate whether viral replication in VCMs was affected when P7-1 tubule formation was inhibited after treatment with dsP7-1, we inoculated VCMs with SRBSDV at an MOI of 10 to guarantee that the early viral infection rate was high. Immunofluorescence microscopy showed no differences in viral infection rate between VCMs that received dsGFP and VCMs that received dsP7-1 at 84 hpi (Fig. 4A). Treatment with dsP7-1 did not significantly reduce the titer of cell-associated viruses, suggesting that RNAi induced by dsP7-1 had no substantial effect on the accumulation of SRBSDV in VCMs (Fig. 4B). Furthermore, the accumulation of P7-1 in dsP7-1-treated VCMs was decreased by about 94% relative to that for the control, as revealed by a Western blotting assay (Fig. 4C). However, the treatment with dsP7-1 did not affect the accumulation of viroplasm matrix protein P9-1 (Fig. 4C). All these results suggest that treatment with dsP7-1 effectively destructs the assembly of P7-1 tubules, leading to the prevention of viral spread among insect vector cells but without interfering with viral replication.

P7-1 tubules directly cross the basal lamina from the initially infected midgut epithelium toward visceral muscle tissues in viruliferous insect vectors. To further investigate the role of P7-1 tubules in viral spread in the insect vector, we used immunofluorescence microscopy to visualize the tubules in the WBPH intestine over the course of viral infection. At 2, 4, and 6 days padp, we immunolabeled the internal organs from 50 WBPHs with P9-1–FITC, P7-1–rhodamine, and the actin dye phalloidin-Alexa Fluor 647 carboxylic acid. The WBPH intestine consists of the anterior diverticulum, esophagus, midgut, and hindgut (10, 20). No specific labeling was detected in the intestine of nonviruliferous WBPHs after immunolabeling with P9-1–FITC and P7-1–rhodamine (Fig. 5A). The intestine of WBPHs is formed by epithelial cells that lie on the basal lamina, which is surrounded by visceral muscle tissues (Fig. 5A). As early as 2 days padp, the initial site for SRBSDV entry and replication in the WBPH was limited to a few epithelial cells of the midgut in 80% of WBPHs tested (Fig. 5B). Unexpectedly, abundant P7-1 tubules extended from the initially infected epithelial cells toward the visceral muscle tissue (Fig. 5B). The visceral muscle tissue of the midgut consists of actin-based internal circular and external longitudinal muscle fibers in WBPHs (Fig. 5). At 2 days padp, immunofluorescence microscopy showed that P7-1 tubules extending from the initially infected epithelial cells were first associated with the internal circular muscle fibers, in which viroplasm containing P9-1 was undetectable (Fig. 5B). At 4 days padp, P7-1 tubules were associated with the external longitudinal muscle fibers, but most of the viroplasms containing P9-1 were restricted to the internal circular muscle tissue in 70% of WBPHs examined (Fig. 5C). At 6 days padp, P7-1 tubules and viroplasms containing P9-1 were extensively associated with the circular and longitudinal muscle tissues throughout the midgut but were undetectable in the epithelium in 70% of WBPHs tested (Fig. 5D). Our previous data revealed that at this time, SRBSDV had spread into the salivary glands (10, 20), suggesting that SRBSDV could directly disseminate into the hemolymph from the visceral muscle tissues and finally into the salivary glands.

We then used electron microscopy to visualize the tubules in the WBPH intestine during infection by SRBSDV. The basal lamina, a noncellular layer lining the epithelium, was covered by visceral muscle tissues (Fig. 6A). At 2 days padp, electron microscopy indicated that SRBSDV infection induced the formation of virus-containing tubules in the midgut epithelial cells (Fig. 6B to G). Theses tubules appeared to be passing through the basal lamina from the infected cell into the visceral muscle tissue (Fig. 6B to G). The tubule was first attached to the matrix of the basal lamina (Fig. 6B and C), and then the entire tubule penetrated through the basal lamina (Fig. 6D to F). Finally, the tubule was released from the basal lamina into the visceral muscle tissue (Fig. 6G). At 6 days padp, electron microscopy indicated that virus-containing tubules were associated with the internal circular or external longitudinal muscle fibers lining the midgut basal lamina (Fig. 7). Furthermore, some of the tubules were associated with the viroplasm (Fig. 7). These tubules appeared to be trafficking along the visceral muscle fibers (Fig. 7), consistent with the observations from im-

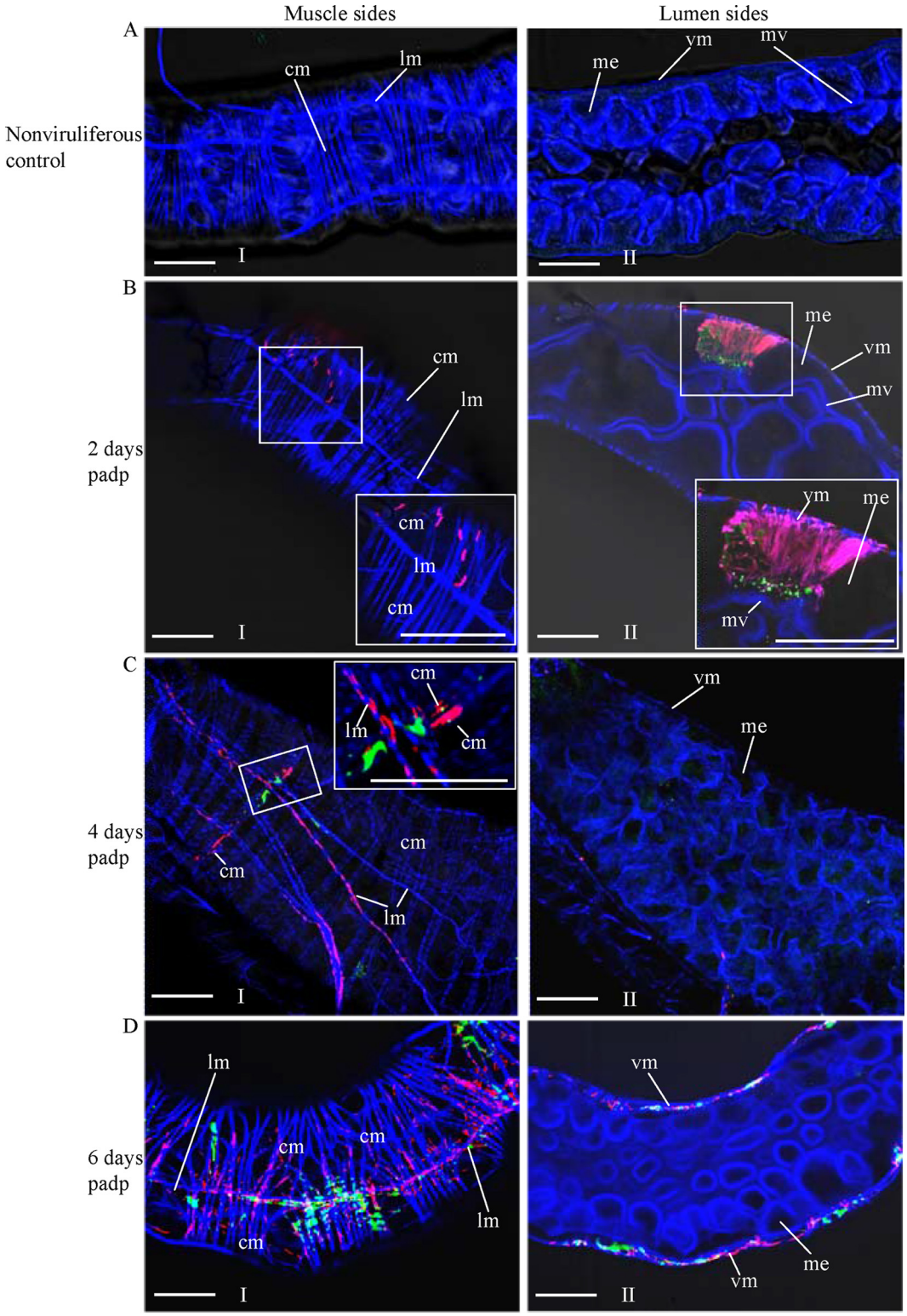

FIG 5 Extension of P7-1 tubules from the initially infected midgut epithelium toward visceral muscle tissues in viruliferous WBPHs. The internal organs of nonviruliferous WBPHs (A) and viruliferous WBPHs at 2 days (B), 4 days (C), or 6 days (D) padp were immunolabeled with P9-1–FITC (green), P7-1–rhodamine (red), and the actin dye phalloidin-Alexa Fluor 647 carboxylic acid (blue) and then examined by confocal microscopy. (Panels I and II) the muscle (I) and lumen (II) sides of the midgut. (Insets) Enlarged images of the boxed areas. Images are representative of those from more than 4 experiments. me, midgut epithelium; mv, microvilli; vm, visceral muscle; cm, circular muscle; lm, longitudinal muscle. Bars, 30 μm.

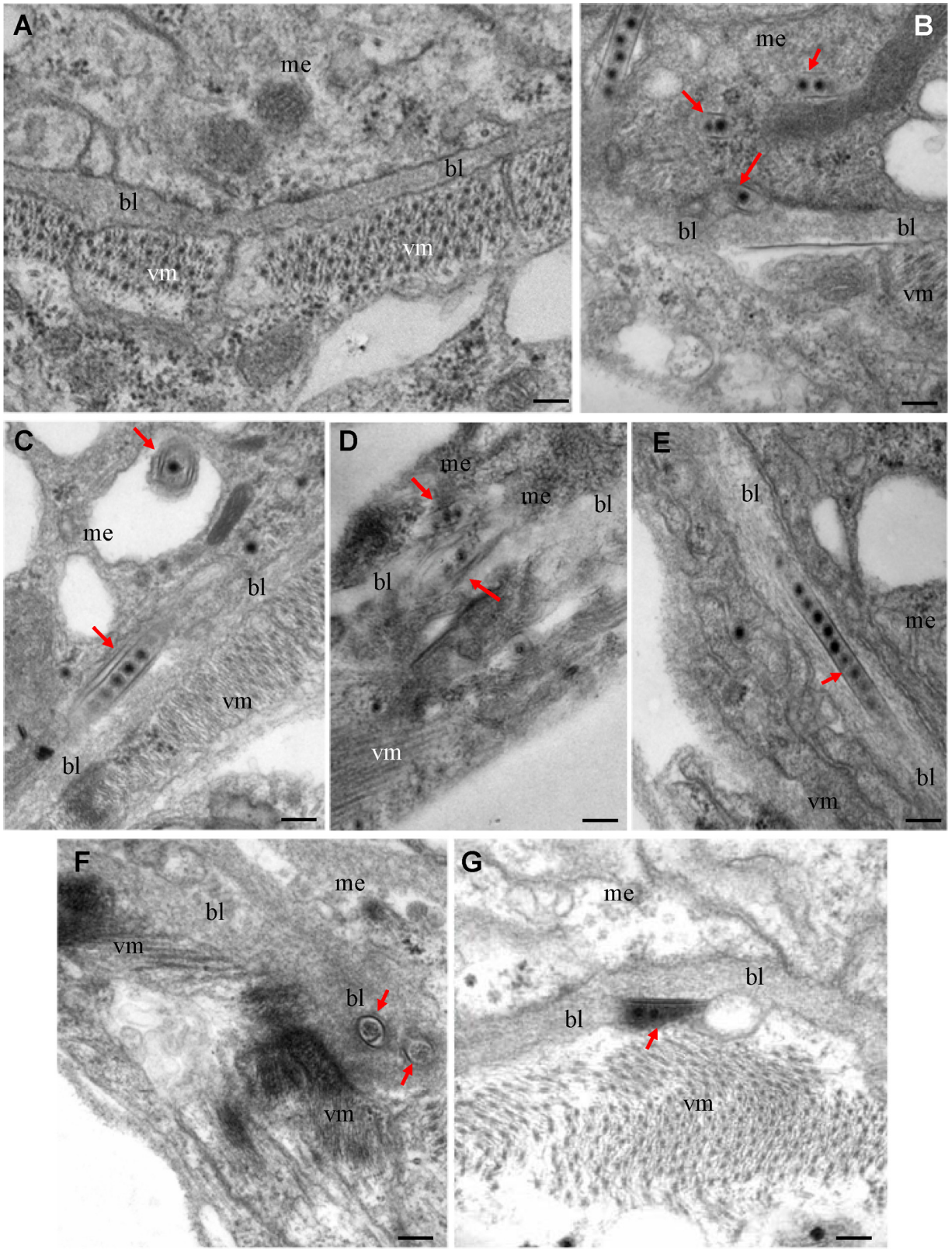

FIG 6 Electron micrographs showing the direct passing of virus-containing tubules through the midgut basal lamina in viruliferous WBPHs at 2 days padp. (A) The midgut of nonviruliferous WBPH; (B, C) the tubules were attached to the basal lamina in the epithelium; (D to F) the entire tubules were completely embedded in the basal lamina in longitudinal (D, E) or transverse (F) sections; (G) the tubule was closely associated with the basal lamina in the visceral muscle tissues. Arrows, virus-containing tubules. bl, basal lamina; me, midgut epithelium; vm, visceral muscle. Bars, 100 nm.

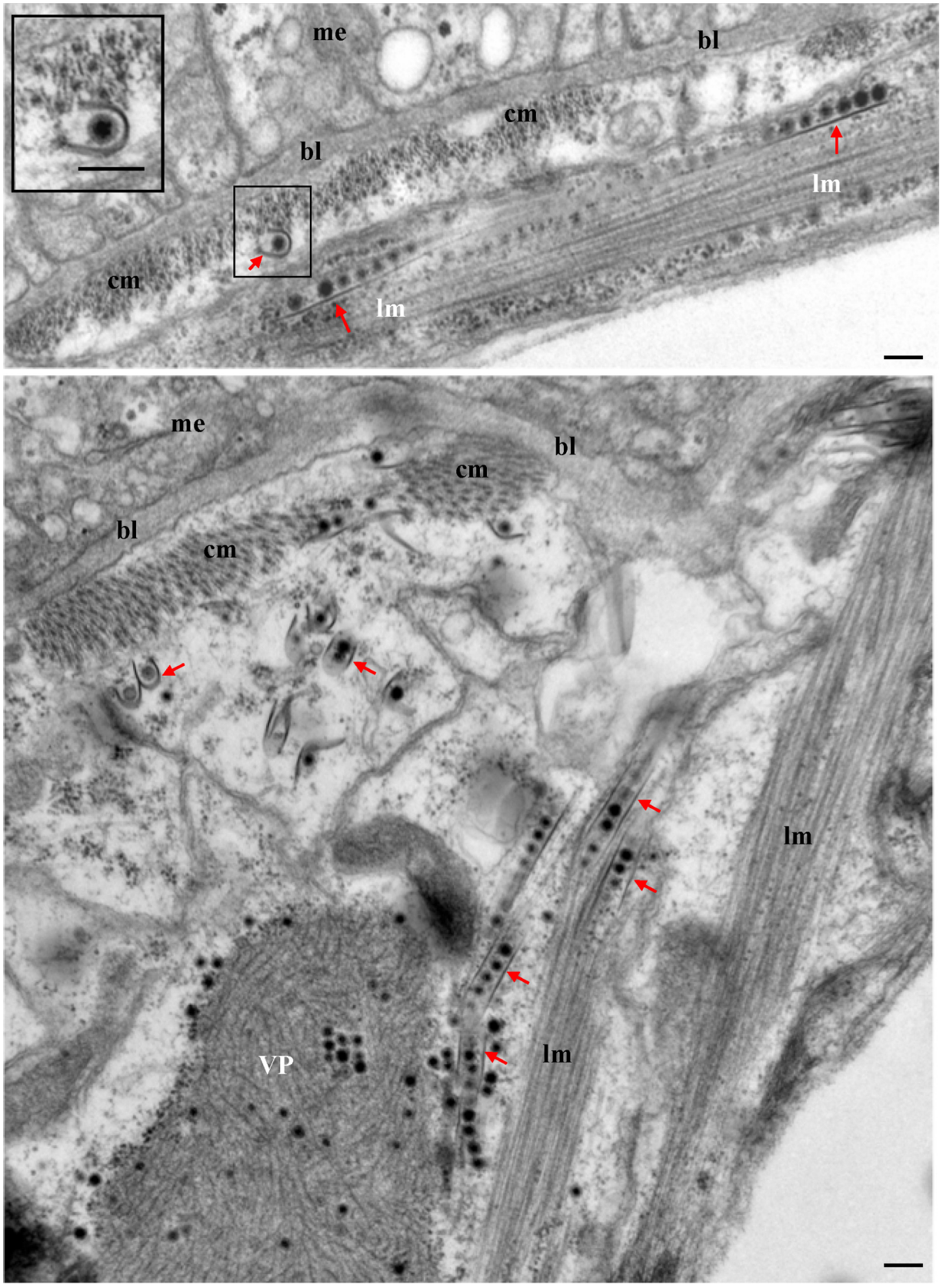

FIG 7 Electron micrographs showing the association of virus-containing tubules with the circular and longitudinal muscle fibers lining the midgut epithelium at 6 days padp. (Inset) Enlarged image of the boxed area. VP, viroplasm; bl, basal lamina; me, midgut epithelium; cm, circular muscle; lm, longitudinal muscle; arrows, virus-containing tubules. Bars, 100 nm.

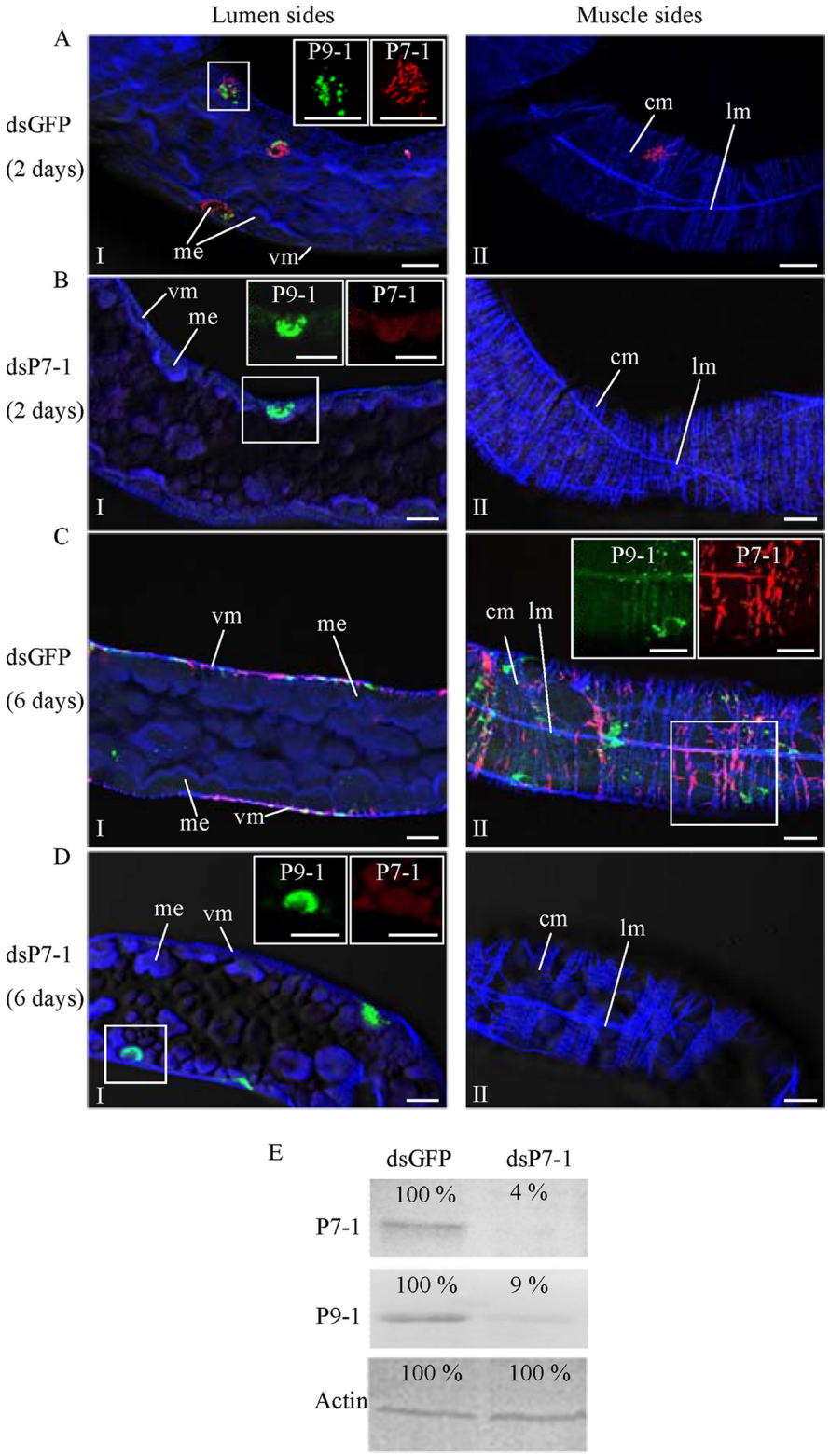

FIG 8 Microinjection of dsP7-1 suppressed viral spread *in vivo* in WBPHs. The nymphs of WBPHs were microinjected with dsGFP (A, C) or dsP7-1 (B, D). At 2 days padp (A, B) or 6 days padp (C, D), the internal organs of WBPHs receiving dsGFP or dsP7-1 were immunolabeled with P9-1–FITC (green), P7-1–rhodamine (red), and the actin dye phalloidin-Alexa Fluor 647 carboxylic acid (blue) and then examined by confocal microscopy. (Panels I and II) The lumen (I) and muscle (II) sides of the midgut. (Insets) Green fluorescence (P9-1 antigens) and red fluorescence (P7-1 antigens) of the merged images in the boxed areas. Images are representative of those from more than 4 experiments. me, midgut epithelium; vm, visceral muscle; cm, circular muscle; lm, longitudinal muscle. Bars, 15 μm. (E) Detection of viral proteins P7-1 and P9-1 in WBPHs by Western blotting assay with P7-1-specific or P9-1-specific IgGs. Insect actin was detected with actin-specific IgG as a control. The protein accumulation level in WBPHs that received dsGFP was taken to be 100%.

TABLE 1 Treatment with dsP7-1 via microinjection suppressed accumulation of SRBSDV *in vivo* and subsequent transmission of SRBSDV by WBPHs

Treatment	Day padp	No. of P7-1- or P9-1-positive insects detected by immunofluorescence in[a]: Limited area of midgut epithelium	Extensive area of midgut visceral muscles	No. of insects that transmitted SRBSDV in expt no.[b]: I	II	III
dsGFP	2	40	0			
	6	0	35			
	15			67	65	70
dsP7-1	2	38	0			
	6	34	0			
	15			0	0	0

[a] Data are for 50 insects.
[b] Data are for 100 insects.

munofluorescence microscopy (Fig. 5). Electron microscopy indicated that SRBSDV particles were packaged in and fixed on the inner surface of the tubules (Fig. 1, 6, and 7). All these results suggest that P7-1 tubules may guide and escort viral particles so that they may spread across the basal lamina into the visceral muscle tissue in the intestine of the viruliferous insect vectors.

The failure of P7-1 tubule formation due to RNAi arrests the spread of SRBSDV from the initially infected epithelium in the viruliferous insect vector. We then tested whether the RNAi induced by microinjection of dsP7-1 could inhibit viral spread in the intestine of WBPHs. At 2 and 6 days padp, we immunolabeled the internal organs from 50 WBPHs that had received dsRNAs with P9-1–FITC, P7-1–rhodamine, and the actin dye phalloidin-Alexa Fluor 647 carboxylic acid. At 2 days padp, viroplasms containing P9-1 were observed in a limited number of the midgut epithelial cells in 80% of WBPHs that received dsGFP or dsP7-1 (Fig. 8A and B; Table 1). However, the treatment with dsP7-1 inhibited the formation of P7-1 tubules in these initially infected midgut epithelial cells (Fig. 8B). At 6 days padp, P7-1 tubules and viroplasms containing P9-1 were seen in the visceral muscle tissues of the midgut in 70% of WBPHs receiving dsGFP (Fig. 8C; Table 1). However, viral infection was still restricted in a limited number of the midgut epithelial cells, in which P7-1 tubule formation was strongly inhibited in 70% of WBPHs receiving dsP7-1 (Fig. 8D; Table 1). The effect of dsP7-1 on the accumulation of P7-1 and P9-1 of SRBSDV was further analyzed by a Western blotting assay with P7-1- and P9-1-specific IgGs, respectively. At 6 days padp, treatment with dsP7-1 caused a more than 90% reduction of P7-1 or P9-1 accumulation in comparison with that for the control (Fig. 8E). Clearly, the treatment of WBPHs with dsP7-1 by microinjection inhibited the transmission of SRBSDV by the insect vectors (Table 1). Taken together, these data suggest that P7-1 tubule formation is essential for the spread of SRBSDV from the epithelium to the visceral muscle tissue in the intestine of the viruliferous insect vectors.

DISCUSSION

Numerous plant viruses are transmitted in a persistent propagative manner by sap-sucking insects, including thrips, aphids, planthoppers, and leafhoppers, but few plant virus-vector systems have been well studied. The limited knowledge of the mechanisms of transmission of these plant viruses by insect vectors is, in part, attributable to the lack of reliable tools for real-time analysis of viruses and virus-induced structures in their vectors. This gap in knowledge can now be bridged with a system that combines the use of insect vector cell cultures, immunofluorescence and electron microscopy, and RNAi assays.

In this study, we investigated how a recently identified plant reovirus, SRBSDV, exploited virus-induced tubules to facilitate viral spread in the bodies of its vector, WBPHs. We first used VCMs derived from WBPHs, an *in vitro* tissue culture system (9, 10), to define the early process of viral spread among insect vector cells. During SRBSDV infection of VCMs, virus-containing tubules were formed and comprised viral nonstructural protein P7-1 (Fig. 1). P7-1 formed tubule-like structures in the absence of viral infection, suggesting that the tubule induced by SRBSDV infection was formed primarily by P7-1 (24). Such P7-1 tubules protruded from the surface of infected cells and penetrated the cytoplasm of neighboring cells (Fig. 1 and 2). Because RNAi induced by dsRNA is a conserved sequence-specific gene-silencing mechanism (25), the synthesized dsRNA targeting the P7-1 gene of SRBSDV could efficiently inhibit P7-1 expression in VCMs (Fig. 3 and 4). Due to the essential role of P7-1 of SRBSDV in the biogenesis of the tubule (24), we thus determined that treatment with dsP7-1 abolished tubule formation and prevented viral spread among insect vector cells but did not affect the replication of SRBSDV in initially infected cells (Fig. 3 and 4). We observed that actin filaments were enclosing P7-1 tubules within the cytoplasm or along the filopodia through a direct interaction of P7-1 and actin (Fig. 2). It appeared that these actin filaments were propelling P7-1 tubules to extend from the surface of infected cells, reminiscent of the actin comet tails that propel the long-distance movement of vaccinia virus (26, 27). These results indicate that SRBSDV could hitch a ride on P7-1 tubules to facilitate viral spread along the actin cytoskeleton in insect vector cells.

The exploitation of P7-1 tubules by SRBSDV for viral spread *in vivo* was determined in our study. Our results show that virus-containing P7-1 tubules were able to protrude from the initially infected epithelium and pass through the basal lamina (Fig. 5 to 7), a finding made for the first time in virus research. This resembles the mode of action by the movement proteins of tubule-forming viruses, such as tomato spotted wilt virus and grapevine fanleaf virus, that increase the size exclusion limit of the plasmodesmata, the tightly regulated channels bridging plant cell walls, to facilitate the transport of virions into neighboring cells (28–30). Thus, virus-induced tubules appear to be an evolved and conserved tool used by plant viruses for overcoming the tightly regulated tissue barriers in insect vectors or plant hosts.

Once the P7-1 tubules crossed the basal lamina, they were associated with the internal circular muscle fibers close to the basal lamina (Fig. 5 and 7). Then, the P7-1 tubules trafficked along the external longitudinal muscle fibers covering the internal circular muscles, leading to the lateral spread of SRBSDV throughout the midgut muscle cells (Fig. 5 and 7). Thus, these actin-based muscle fibers, reminiscent of actin filaments enclosing the P7-1 tubules in the cultured WBPH cells, may propel the long-distance movement of the P7-1 tubules via actin polymerization (31, 32). SRBSDV is apparently disseminated directly from the visceral muscle tissues into the hemocoel and then into the salivary glands

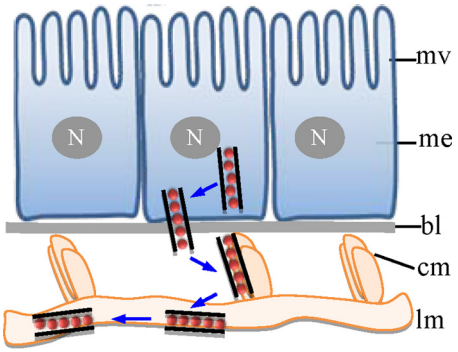

FIG 9 Proposed model for the trafficking of P7-1 tubules *in vivo* in its insect vector, WBPH. Virus-containing P7-1 tubules pass across the basal lamina from the initially infected midgut epithelium, traffic along the internal circular muscle tissues, and then spread through the external longitudinal muscle tissues. bl, basal lamina; me, midgut epithelium; mv, microvilli; cm, circular muscle; lm, longitudinal muscle; N, nucleus.

(10, 20). Recently, P7-1 of SRBSDV has been demonstrated to specifically interact with six proteins of WBPHs, including neuroglian, myosin light chain 2, polyubiquitin, E3 ubiquitin ligase, ribophorin II, and profilin (33). How these insect proteins are involved in the movement of P7-1 tubules in the body of the insect vector remains to be further investigated. In this study, we show that the failure of P7-1 tubule formation as a result of RNAi induced by synthesized dsRNA targeting the P7-1 gene inhibited the spread of SRBSDV from the initially infected epithelium toward the visceral muscles (Fig. 8), further supporting the assumption that SRBSDV exploits P7-1 tubules to spread from the midgut epithelium into visceral muscle tissues through the basal lamina in its insect vector. Based on discussion presented above, we propose a model for the trafficking of P7-1 tubules *in vivo* (Fig. 9). In this model, virus-induced tubule serves as a vehicle for virions to pass through the basal lamina from the initially infected midgut epithelium, traffic along the internal circular visceral muscle tissues, and then pass through the external longitudinal muscle tissues (Fig. 9). To our knowledge, this represents the first elucidation of the mechanism for the rapid dissemination of virus from the intestine to the hemolymph in hemipteran insects.

In cultured cells of vertebrate animals, several animal viruses can induce various intercellular channels, such as filopodia, membrane nanotubes, and virological synapses, and thus enable cell-to-cell spread in the host (34, 35). An important caveat is that most of our current knowledge about the mechanisms for intercellular spread of animal viruses is derived from *in vitro* studies; how these mechanisms relate to infected vertebrate animals *in vivo* is unknown. Here, we demonstrate that virus-induced tubule can serve as a vehicle for viral spread in insect vectors, the invertebrate animals from *in vitro* and *in vivo* studies. The tracheal system has been proposed to be a vehicle for baculoviruses to pass from the intestine through the basal lamina in lepidopteran insects (36, 37). Despite the divergence between virus-induced tubule and the tracheal system, they still have similar tubular morphologies and similar functions in mediating viral transport across the basal lamina from the intestine. Thus, viruses have evolved to exploit virus-induced or insect-derived conduits to escape across the basal lamina from the intestine.

Previously, we demonstrated that RDV, a phytoreovirus of the plant reoviruses, exploits virus-containing tubules composed of the nonstructural protein Pns10 to pass through microvilli of the midgut epithelium into the lumen (13). Furthermore, Pns10 tubules of RDV are never found in association with the basal lamina (13). However, in the case of SRBSDV, virus-containing P7-1 tubules do not traverse the microvilli and instead directly cross the basal lamina from the initially infected midgut epithelium. Thus, Pns10 tubules of RDV may confer a selective advantage for the cell-to-cell spread of virus among midgut epithelial cells in the leafhopper vector (12, 13), while P7-1 tubules of SRBSDV are empowered for the direct, and thus more rapid, spread of the virus from the epithelial cells to the hemocoel and salivary glands in its vector. This suggestion is consistent with the fact that the latent period for SRBSDV in its insect vector ranges from 6 to 9 days; in contrast, it is 2 to 3 weeks for RDV (16, 18, 38). These analyses suggest that SRBSDV, a recently identified plant reovirus, has evolved to be well adapted for persistent transmission by its WBPH vector.

ACKNOWLEDGMENTS

This research was supported by the National Natural Science Foundation of China (31130044), the National Basic Research Program of China (2014CB138400), the National Science Foundation for Outstanding Youth (31325023), and a project from the Henry Fok Education Foundation (131019).

REFERENCES

1. **Ammar ED.** 1985. Internal morphology and ultrastructure of leafhoppers and planthoppers, p 121–162. *In* Nault LR, Rodriguez JG (ed), Leafhoppers and planthoppers. John Wiley & Sons, Brisbane, Australia.
2. **Cheung WWK, Purcell AH.** 1993. Ultrastructure of the digestive system of the leafhopper *Euscelidius variegatus* Kirshbaum (Homoptera: Cicadellidae), with and without congenital bacterial infections. Int. J. Insect Morphol. Embryol. **22:**49–61. http://dx.doi.org/10.1016/0020-7322(93)90033-W.
3. **Hogenhout SA, Ammar E-D, Whitfield AE, Redinbaugh MG.** 2008. Insect vector interactions with persistently transmitted viruses. Annu. Rev. Phytopathol. **46:**327–359. http://dx.doi.org/10.1146/annurev.phyto.022508.092135.
4. **Ammar ED, Tsai CW, Whitfield AE, Redinbaugh MG, Hogenhout SA.** 2009. Cellular and molecular aspects of rhabdovirus interactions with insect and plant hosts. Annu. Rev. Entomol. **54:**447–468. http://dx.doi.org/10.1146/annurev.ento.54.110807.090454.
5. **Bragard C, Caciagli P, Lemaire O, Lopez-Moya JJ, MacFarlane S, Peters D, Susi P, Torrance L.** 2013. Status and prospects of plant virus control through interference with vector transmission. Annu. Rev. Phytopathol. **51:**177–201. http://dx.doi.org/10.1146/annurev-phyto-082712-102346.
6. **Wei T, Shimizu T, Hagiwara K, Kikuchi A, Moriyasu Y, Suzuki N, Chen H, Omura T.** 2006. Pns12 protein of *Rice dwarf virus* is essential for formation of viroplasms and nucleation of viral-assembly complexes. J. Gen. Virol. **87:**429–438. http://dx.doi.org/10.1099/vir.0.81425-0.
7. **Chen H, Zheng L, Mao Q, Liu Q, Jia D, Wei T.** 2014. Development of continuous cell culture of brown planthopper to trace the early infection process of oryzaviruses in insect vector cells. J. Virol. **88:**4265–4274. http://dx.doi.org/10.1128/JVI.03466-13.
8. **Jia D, Guo N, Chen H, Akita F, Xie L, Omura T, Wei T.** 2012. Assembly of the viroplasm by viral non-structural protein Pns10 is essential for persistent infection of rice ragged stunt virus in its insect vector. J. Gen. Virol. **93:**2299–2309. http://dx.doi.org/10.1099/vir.0.042424-0.
9. **Mao Q, Zheng S, Han Q, Chen H, Ma Y, Jia D, Chen Q, Wei T.** 2013. New model for the genesis and maturation of viroplasms induced by fijiviruses in insect vector cells. J. Virol. **87:**6819–6828. http://dx.doi.org/10.1128/JVI.00409-13.
10. **Jia D, Chen H, Zheng A, Chen Q, Liu Q, Xie L, Wu Z, Wei T.** 2012. Development of an insect vector cell culture and RNA interference system to investigate the functional role of fijivirus replication protein. J. Virol. **86:**5800–5807. http://dx.doi.org/10.1128/JVI.07121-11.

11. **Wu W, Zheng L, Chen H, Jia D, Li F, Wei T.** 2014. Nonstructural protein NS4 of *Rice stripe virus* plays a critical role in viral spread in the body of vector insects. PLoS One **9:**e88636. http://dx.doi.org/10.1371/journal.pone.0088636.
12. **Chen H, Chen Q, Omura T, Uehara-Ichiki T, Wei T.** 2011. Sequential infection of *Rice dwarf virus* in the internal organs of its insect vector after ingestion of virus. Virus Res. **160:**389–394. http://dx.doi.org/10.1016/j.virusres.2011.04.028.
13. **Chen Q, Chen H, Mao Q, Liu Q, Shimizu T, Uehara-Ichiki T, Wu Z, Xie L, Omura T, Wei T.** 2012. Tubular structure induced by a plant virus facilitates viral spread in its vector insect. PLoS Pathog. **8:**e1003032. http://dx.doi.org/10.1371/journal.ppat.1003032.
14. **Wei T, Kikuchi A, Moriyasu Y, Suzuki N, Shimizu T, Hagiwara K, Chen H, Takahashi M, Ichiki-Uehara T, Omura T.** 2006. The spread of *Rice dwarf virus* among cells of its insect vector exploits virus-induced tubular structures. J. Virol. **80:**8593–8602. http://dx.doi.org/10.1128/JVI.00537-06.
15. **Chen H, Zheng L, Jia D, Zhang P, Chen Q, Liu Q, Wei T.** 2013. Rice gall dwarf virus exploits tubules to facilitate viral spread among cultured insect vector cells derived from leafhopper Recilia dorsalis. Front. Microbiol. **4:**206. http://dx.doi.org/10.3389/fmicb.2013.00206.
16. **Zhou GH, Wen JJ, Cai DJ, Li P, Xu DL, Zhang SG.** 2008. Southern rice black-streaked dwarf virus: a new proposed *Fijivirus* species in the family *Reoviridae*. Chin. Sci. Bull. **53:**3677–3685. http://dx.doi.org/10.1007/s11434-008-0467-2.
17. **Wang Q, Yang J, Zhou GH, Zhang HM, Chen JP, Adams MJ.** 2010. The complete genome sequence of two isolates of southern rice black-streaked dwarf virus, a new member of the genus *Fijivirus*. J. Phytopathol. **158:**733–737. http://dx.doi.org/10.1111/j.1439-0434.2010.01679.x.
18. **Pu LL, Xie GH, Ji CY, Ling B, Zhang MX, Xu DL, Zhou GH.** 2012. Transmission characteristics of southern rice black-streaked dwarf virus by rice planthoppers. Crop Prot. **41:**71–76. http://dx.doi.org/10.1016/j.cropro.2012.04.026.
19. **Hoang AT, Zhang HM, Yang J, Chen JP, Hebrard E, Zhou GH, Vinh VN, Cheng JA.** 2011. Identification, characterization, and distribution of southern rice black-streaked dwarf virus in Vietnam. Plant Dis. **95:**1063–1069. http://dx.doi.org/10.1094/PDIS-07-10-0535.
20. **Jia D, Chen H, Mao Q, Liu Q, Wei T.** 2012. Restriction of viral dissemination from the midgut determines incompetence of small brown planthopper as a vector of southern rice black-streaked dwarf virus. Virus Res. **167:**404–408. http://dx.doi.org/10.1016/j.virusres.2012.05.023.
21. **Miyazaki N, Uehara-Ichiki T, Xing L, Bergman L, Higashiura A, Nakagawa A, Omura T, Cheng RH.** 2008. Structural evolution of reoviridae revealed by oryzavirus in acquiring the second capsid shell. J. Virol. **82:**11344–11353. http://dx.doi.org/10.1128/JVI.02375-07.
22. **Kimura I.** 1986. A study of rice dwarf virus in vector cell monolayers by fluorescent antibody focus counting. J. Gen. Virol. **67:**2119–2124. http://dx.doi.org/10.1099/0022-1317-67-10-2119.
23. **Liu S, Ding Z, Zhang C, Yang B, Liu Z.** 2010. Gene knockdown by intro-thoracic injection of double-stranded RNA in the brown planthopper, *Nilaparvata lugens*. Insect Biochem. Mol. Biol. **40:**666–671. http://dx.doi.org/10.1016/j.ibmb.2010.06.007.
24. **Liu Y, Jia D, Chen H, Chen Q, Xie L, Wu Z, Wei T.** 2011. The P7-1 protein of southern rice black-streaked dwarf virus, a fijivirus, induces the formation of tubular structures in insect cells. Arch. Virol. **156:**1729–1736. http://dx.doi.org/10.1007/s00705-011-1041-9.
25. **Fire A, Xu S, Montgomery MK, Kostas SA, Driver SE, Mello CC.** 1998. Potent and specific genetic interference by double-stranded RNA in *Caenorhabditis elegans*. Nature **391:**806–811. http://dx.doi.org/10.1038/35888.
26. **Cudmore S, Cossart P, Griffiths Way GM.** 1995. Actin-based motility of vaccinia virus. Nature **378:**636–638. http://dx.doi.org/10.1038/378636a0.
27. **Doceul V, Hollinshead M, van der Linden L, Smith GL.** 2010. Repulsion of superinfecting virions: a mechanism for rapid virus spread. Science **327:**873–876. http://dx.doi.org/10.1126/science.1183173.
28. **Li W, Lewandowski DJ, Hilf ME, Adkins S.** 2009. Identification of domains of the tomato spotted wilt virus NSm protein involved in tubule formation, movement and symptomatology. Virology **390:**110–121. http://dx.doi.org/10.1016/j.virol.2009.04.027.
29. **Amari K, Boutant E, Hofmann C, Schmitt-Keichinger C, Fernandez-Calvino L, Didier P, Lerich A, Mutterer J, Thomas CL, Heinlein M, Mély Y, Maule AJ, Ritzenthaler C.** 2010. A family of plasmodesmal proteins with receptor-like properties for plant viral movement proteins. PLoS Pathog. **6:**e1001119. http://dx.doi.org/10.1371/journal.ppat.1001119.
30. **Amari K, Lerich A, Schmitt-Keichinger C, Dolja VV, Ritzenthaler C.** 2011. Tubule-guided cell-to-cell movement of a plant virus requires class XI myosin motors. PLoS Pathog. **7:**e1002327. http://dx.doi.org/10.1371/journal.ppat.1002327.
31. **Cameron LA, Footer MJ, van Oudenaarden A, Theriot JA.** 1999. Motility of ActA protein-coated microspheres driven by actin polymerization. Proc. Natl. Acad. Sci. U. S. A. **27:**4908–4913.
32. **Baluska F, Hlavacka A, Volkmann D, Menzel D.** 2004. Getting connected: actin-based cell-to-cell channels in plants and animals. Trends Cell Biol. **14:**404–408. http://dx.doi.org/10.1016/j.tcb.2004.07.001.
33. **Mar T, Liu W, Wang X.** 2014. Proteomic analysis of interaction between P7-1 of southern rice black-streaked dwarf virus and the insect vector reveals diverse insect proteins involved in successful transmission. J. Proteomics **102:**83–97. http://dx.doi.org/10.1016/j.jprot.2014.03.004.
34. **Sattentau QJ.** 2011. The direct passage of animal viruses between cells. Curr. Opin. Virol. **1:**396–402. http://dx.doi.org/10.1016/j.coviro.2011.09.004.
35. **Ritzenthaler C.** 2011. Parallels and distinctions in the direct cell-to-cell spread of the plant and animal viruses. Curr. Opin. Virol. **1:**403–409. http://dx.doi.org/10.1016/j.coviro.2011.09.006.
36. **Engelhard EK, Kam-Morgan LN, Washburn JO, Volkman LE.** 1994. The insect tracheal system: a conduit for the systemic spread of Autographa californica M nuclear polyhedrosis virus. Proc. Natl. Acad. Sci. U. S. A. **91:**3224–3227. http://dx.doi.org/10.1073/pnas.91.8.3224.
37. **Means JC, Passarelli AL.** 2010. Viral fibroblast growth factor, matrix metalloproteases, and caspases are associated with enhancing systemic infection by baculoviruses. Proc. Natl. Acad. Sci. U. S. A. **107:**9825–9830. http://dx.doi.org/10.1073/pnas.0913582107.
38. **Honda K, Wei T, Hagiwara K, Higashi T, Kimura I, Akutsu K, Omura T.** 2007. Retention of rice dwarf virus by descendants of pairs of viruliferous vector insects after rearing for 6 years. Phytopathology **97:**712–716. http://dx.doi.org/10.1094/PHYTO-97-6-0712.